arXiv:cond-mat/0204287v1 [cond-mat.mes-hall] 12 Apr 2002

Superconducting Single-Electron Transistor in a Locally Tunable Electromagnetic Environment: Dissipation and Charge Fluctuations

W. Lu,[1] K. D. Maranowski,[2] and A. J. Rimberg[1,3]

[1]*Department of Physics and Astronomy, Rice University, Houston, Texas 77005*
[2]*Materials Department, University of California, Santa Barbara, California 93106**
[3]*Department of Electrical and Computer Engineering, Rice University, Houston, Texas 77005*

We have developed a novel system consisting of a superconducting single-electron transistor (S-SET) coupled to a two-dimensional electron gas (2DEG), for which the dissipation can be tuned in the immediate vicinity of the S-SET. Within linear response, the S-SET conductance varies nonmonotonically with increasing 2DEG impedance. We find good agreement between our experimental results and a model incorporating electromagnetic fluctuations in both the S-SET leads and the 2DEG, as well as low-frequency switching of the S-SET offset charge.

PACS numbers: 74.50.+r,73.23.Hk,74.40.+k

Electrical transport in nanoscale devices is strongly affected by the electromagnetic properties of their environment. This is particularly true for superconducting systems, and has been a topic of considerable interest lately: dissipation can drive a superconductor-insulator quantum phase transition [1, 2, 3], and is also expected to affect the coherence time of qubits such as the charge-based single Cooper pair box [4, 5, 6]. Maintaining quantum coherence in such devices long enough to allow many operations is prerequisite for their use in quantum computation. In this regard, the closely related superconducting single electron transistor (S-SET) is an excellent system for attaining a better understanding of the effects of the electromagnetic environment on quantum coherence.

This approach was followed by the Berkeley group [7], who fabricated an S-SET above a two-dimensional electron gas (2DEG) in a GaAs/Al_xGa_{1-x}As heterostructure. Using a back gate to vary the 2DEG sheet resistance R_{sq} they measured changes in the S-SET conductance $G_{\rm SET}$ as the dissipation was varied. Building on earlier theoretical work [8, 9, 10, 11, 12], Wilhelm, *et al.* predicted [13] that within linear response $G_{\rm SET}$ would scale with the ground plane conductance $G_{\rm 2D} = 1/R_{sq}$ and temperature T as $G_{\rm 2D}^{\beta}/T^{\alpha}$ and that the S-SET current I at fixed bias voltage V would vary *nonmonotonically* with $G_{\rm 2D}$, while switching from the non-linear to linear regime. These predictions were made within two models: in one the environment was treated as a ground plane, while in the other it was treated as an infinite *RC* transmission line provided by the SET leads. While the Berkeley group did observe power law behavior, their measured exponents were not in quantitative agreement with theory. Furthermore, the measured β depended on T and α on $G_{\rm 2D}$, calling the scaling form into question.

In this Letter, we report measurements on samples similar to those studied by the Berkeley group; in our samples, however, we can modify $G_{\rm 2D}$ in the immediate vicinity of the S-SET while leaving the 2DEG beneath the leads largely untouched. In contrast to the predictions of Wilhelm, *et al.* we observe a nonmonotonic dependence of $G_{\rm SET}$ on $G_{\rm 2D}$ entirely within the linear regime. We propose a model for the environmental impedance of S-SET/2DEG systems that includes electromagnetic fluctuations in both the 2DEG and leads, while treating the latter as *finite RC* transmission lines. We also allow for relatively low-frequency switching of the charge state of the SET island[14], which can affect the measured current. Within this model, we find good agreement between our calculated and measured results.

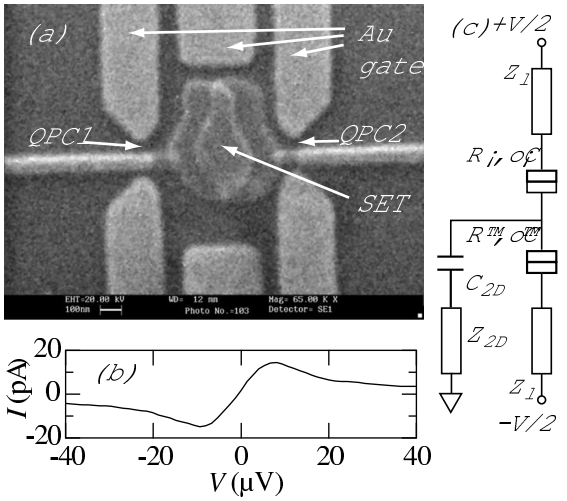

FIG. 1: (a) Electron micrograph showing the S-SET, gold gates, and QPCs. (b) S-SET *I*-*V* characteristics for $V_g = 0$. The linear regime extends to roughly ± 8 μV. (c) Circuit diagram of the S-SET, including its environment. We allow both for lead impedances Z_ℓ and a ground impedance $Z_{\rm 2D}$ coupled to the S-SET through a capacitance $C_{\rm 2D}$.

An electron micrograph of a typical sample is shown in Fig. 1(a). We begin with an GaAs/Al_xGa_{1-x}As heterostructure grown on a GaAs substrate using molecular beam epitaxy, consisting of the following layers: 1000 nm of GaAs, 47 nm of $Al_{0.3}Ga_{0.7}As$ and 5 nm of GaAs. The $Al_{0.3}Ga_{0.7}As$ is delta-doped with Si 22 nm from

the lower GaAs/$Al_{0.3}Ga_{0.7}As$ interface, at which forms a two-dimensional electron gas (2DEG) with $R_{sq} = 20\ \Omega$ and sheet density $n_s = 3.6 \times 10^{11}$ cm^{-2}. On the sample surface we use electron-beam lithography and shadow evaporation to fabricate an Al/AlO_x S-SET surrounded by six Au gates [15]. When no gate voltage is applied and the 2DEG is unconfined, the measured I-V characteristics are linear over several microvolts, as shown in Fig. 1(b). We can also apply a single gate voltage V_g to any combination of Au gates, excluding the 2DEG beneath them. We focus on two geometries: the "pool," in which all six gates are energized, and the "stripe" in which only the four exterior gates are. In both cases, electrons immediately beneath the SET are coupled to ground by quantum point contacts (QPCs) with conductances $1/R_{\rm QPC}$ (assumed equal) as low as 3 conductance quanta $G_0 = e^2/h$. In the stripe geometry, the electrons can also move vertically through a resistance $R_{\rm str}$ to a large 2DEG reservoir that is coupled to ground through a capacitance $C_{\rm str}$. As illustrated in Fig. 1(c), electromagnetic fluctuations in the environment can couple to the tunneling electrons in two ways: through the leads, which act as RC transmission lines with impedance Z_ℓ for the relevant frequency range [7, 13], and through the capacitance $C_{\rm 2D}$ to the 2DEG with impedance $Z_{\rm 2D}$, which is related to $R_{\rm QPC}$ and (for the stripe) $R_{\rm str}$. The model has been studied previously [16, 17] without considering particular forms for $Z_{\rm 2D}$ and Z_ℓ.

Measurements were performed on two separate samples (S1 and S2) in a dilution refrigerator in a four-probe voltage biased configuration; the estimated electron temperature was 100 mK. High frequency noise was excluded using standard techniques. A small capacitance $C_g \approx 20.3$ aF (not shown in Fig. 1(c)) couples the six Au gates to the S-SET. The other sample parameters such as the junction resistances $R_{1,2}$ and capacitances $C_{1,2}$, the coupling capacitance $C_{\rm 2D}$ and superconducting gap Δ are given elsewhere [18]. The charging energy $E_c = e^2/2C_\Sigma$ for sample S1 (S2) is 118 (77) μeV while the Josephson energy $E_{J_j} = \frac{R_Q}{2R_j}\Delta$ averaged for the two junctions is 4.7 (21.8) μeV. Here $R_Q = \frac{h}{4e^2}$ is the superconducting resistance quantum and $C_\Sigma = C_1 + C_2 + C_{\rm 2D} + C_g$. We use standard lock-in techniques and voltage biases of 3 and 5 μV rms respectively to measure $G_{\rm SET}$ and the conductance $G_{\rm 2D}$ across the series combination of the QPCs versus V_g in the pool and stripe geometries. The results for S2 are shown in Fig. 2.

From Fig. 2(b), we see that for the pool $G_{\rm SET}$ rises by nearly a factor of 2 as V_g becomes more negative, before dropping rapidly. Although $G_{\rm 2D}$ vs. V_g is nearly identical in both cases, $G_{\rm SET}$ for the stripe rises only by $\sim$50% and does not decrease, even for the most negative V_g. In both plots, e-periodic Coulomb blockade oscillations are seen as the S-SET offset charge varies. We fit a smoothly varying function to the measured $G_{\rm 2D}$ versus V_g (inset,

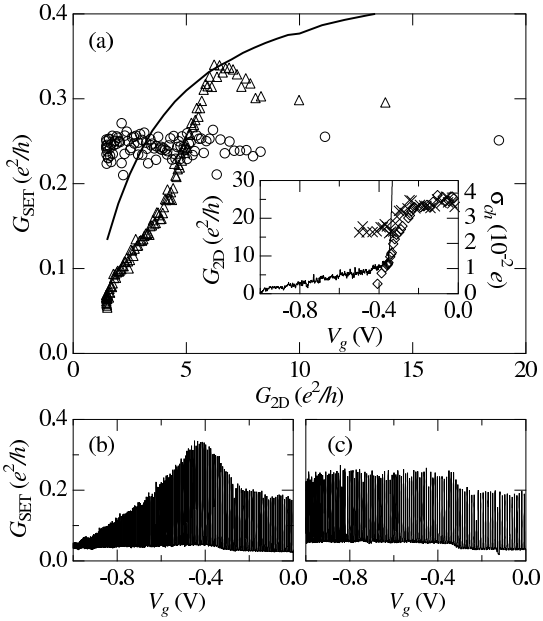

FIG. 2: (a) Maxima of $G_{\rm SET}$ vs. $G_{\rm 2D}$ in the stripe ($\circ$) and pool ($\triangle$) geometries. Solid line: $G^c_{\rm SET}$vs. $G_{\rm 2D}$. Inset: $G_{\rm 2D}$ (solid line) for the pool, and σ_{ch} in the stripe ($\times$) and pool ($\diamond$) geometries vs. V_g. (b) $G_{\rm SET}$ vs. V_g in the pool geometry. (c) $G_{\rm SET}$ vs. V_g in the stripe geometry.

Fig. 2(a)) which we use to plot the maxima of $G_{\rm SET}$ versus $G_{\rm 2D}$ in Fig. 2(a). The knee in $G_{\rm 2D}$ at $V_g \approx -0.38$ V corresponds to the appearance of quantized plateaux in the individual QPC conductances.

To understand these results and the I-V curve in Fig. 1 (b), we begin with the rate of sequential Cooper pair tunneling [19] through junction j, valid for $E_J \ll E_c$

$$\Gamma(\delta f^{(j)}) = (\pi/2\hbar)E_{J_j}^2 P(-\delta f^{(j)}) \qquad (1)$$

where $\delta f^{(j)} = f_f - f_i = (-1)^j 4E_c(2N - n_g + 1) - 2\alpha_j eV$ is the free energy difference for changing the number of Cooper pairs N by 1, $\alpha_j = \frac{1}{2} + (-1)^j(C_1 - C_2)/2C_\Sigma$, and $n_g = C_g V_g/e$. Here P(E) is the probability of exchanging energy E with the environment and can be expressed in terms of a correlation function $K(t) = R_Q^{-1}\int_{-\infty}^{\infty}\frac{d\omega}{\omega}{\rm Re}[Z_t(\omega)]\{\coth(\frac{\hbar\omega}{2k_BT})[\cos(\omega t) - 1] - i\sin(\omega t)\}$ via $P(E) = \frac{1}{2\pi\hbar}\int_{-\infty}^{\infty} dt\ \exp[K(t) + i\frac{Et}{\hbar}]$ where $Z_t(\omega)$ is the total impedance seen by tunneling electrons.

The general result for $Z_t(\omega)$ within the model of Fig. 1(c) is quite complex [17]. In our case, however, Z_ℓ ($Z_{\rm 2D}$) dominates at low (high) frequencies and to an excellent approximation

$${\rm Re}[Z_t(\omega)] = \kappa_1 {\rm Re}[Z_\ell(\omega)] + \frac{\kappa_2 Z_{\rm 2D}}{1 + [\omega C_{\rm eff}\kappa_2 Z_{\rm 2D}]^2} \qquad (2)$$

where for junction 1(2) $\kappa_1 = \frac{(C_{2(1)}+C_{\rm 2D})^2 + C_{2(1)}^2}{C_\Sigma^2}$, $\kappa_2 = (\frac{C_{\rm 2D}}{C_\Sigma})^2$, $C_{\rm eff} = \frac{(C_1+C_2)C_\Sigma}{C_{\rm 2D}}$ and we treat $Z_{\rm 2D}$ as a resistance. For Z_ℓ we begin with the impedance of a *finite RC*

line $Z_{RC}(\omega) = \sqrt{\frac{r_\ell}{i\omega c_\ell}}\tanh(\sqrt{i\omega r_\ell c_\ell \ell^2})$ where r_ℓ and c_ℓ are the resistance and capacitance per unit length and ℓ is the total line length. We are interested in the long-time limit of $K(t)$ which is dominated by the low-frequency part of $Z_t(\omega)$. In that limit, $Z_{RC}(\omega) \approx \frac{r_\ell \ell}{1+(\omega r_\ell c_\ell \ell^2/\sqrt{6})^2}$, which we use for Z_ℓ in Eq. 2.

A detailed analysis of $K(t)$ will be given elsewhere. Here we note that both parts of $Z_t(\omega)$ in Eq. 2 have the same form. For Z_{2D}, the corner frequency $\omega_c = 1/(C_{\rm eff}\kappa_2 Z_{2D})$ satisfies $\hbar\omega_c \gg k_BT$ and we may use the kernel of Ref. 13, while for Z_{RC} we find that $\omega_c = \sqrt{6}/r_\ell c_\ell \ell^2$ usually satisfies $\hbar\omega_c \ll k_BT$ and requires different treatment. Since $K(t)$ is linear in $\mathrm{Re}[Z_t(\omega)]$, we may calculate $K(t)$ and $P(E)$ separately for Z_{2D} and Z_ℓ and find the total $P_{\rm tot}(E)$ as a convolution. For Z_{2D}, then, we have $P_{2D}(E) = \frac{(2\pi\kappa_2 C_{\rm eff} Z_{2D} k_BT/\hbar)^{2\kappa_2/g}}{2\pi^2 k_BT}\mathrm{Re}[e^{-i\pi\kappa_2/g}B(\frac{\kappa_2}{g}-\frac{iE}{2\pi k_BT}, 1-\frac{2\kappa_2}{g})]$ where $g = R_Q/Z_{2D}$ and $B(x,y)$ is the beta function [13]. For Z_{RC}, we find that

$$K_{RC}(t) = -\frac{2\kappa_1}{g_{rc}}\Big\{\pi k_BT|t|/\hbar + \frac{\pi}{2}[\cot(\frac{\hbar g_{rc}}{2k_BT\tau}) - i\mathrm{sign}(t)](e^{-|t|/\tau}-1)\Big\} \quad (3)$$

is valid for $\frac{\hbar g_{rc}}{2k_BT\tau} \lesssim \pi/2$, where $g_{rc} = R_Q/(r_\ell\ell)$ and $\tau = R_Q c_\ell \ell/\sqrt{6}$. From this we calculate

$$P_{RC}(E) = \frac{\tau}{\pi g_{rc}\hbar}e^{\gamma_3(g_{rc})}\mathrm{Re}\big[e^{-i\frac{\kappa_1\pi}{g_{rc}}}\gamma_2(g_{rc})^{-\gamma_1(g_{rc})} \times\{\Gamma[\gamma_1(g_{rc})] - \Gamma[\gamma_1(g_{rc}),\gamma_2(g_{rc})]\}\big] \quad (4)$$

where $\gamma_1(g) = \frac{2\pi\kappa_1 k_BT\tau}{\hbar g^2} - iE\tau/\hbar g$, $\gamma_2(g) = \gamma_3(g) - i\pi\kappa_1/g$, $\gamma_3(g) = \frac{\kappa_1\pi}{g}\cot\left(\frac{\hbar g}{2k_BT\tau}\right)$ and $\Gamma(x,y)$ is the incomplete gamma function.

To proceed we need an accurate model of $Z_t(\omega)$. For the $V_g = 0$ I-V curve to be linear at $V \approx 8$ μV, Z_t/R_Q must be nonnegligible at frequencies of order $eV/h \approx 2$ GHz. Since then $Z_{2D} \approx R_{sq} = 20\ \Omega$, Z_ℓ must dominate Z_t for small Z_{2D}. We therefore consider the structure of our leads, which vary in width w from 100 nm to 20 μm. The 100 nm section has length $\ell = 1$ μm, contributes only 50 Ω to $Z_\ell(0)$, and is not considered further. For the remaining sections with $w = 0.4$, 1.0, 10 and 20 μm, and $\ell = 9$, 57, 253 and 375 μm we use $r_\ell \approx R_{sq}/(w+5.8h)$ and $c_\ell \approx \varepsilon\varepsilon_0(w/h+1.393)$ where $h = 50$ nm is the 2DEG depth and $\varepsilon = 13$ the dielectric constant of GaAs to calculate $r_\ell = 29$, 16, 1.9 and 1.0 MΩ/m and $c_\ell = 1.1$, 2.5, 23 and 46 nF/m. These four sections form a cascaded RC line which determines $Z_\ell(\omega)$. The total $Z_t(\omega)$ calculated from Eq. 2 is shown for different values of $Z_{2D} = 1/(4G_{2D})$ for the pool geometry in Fig. 3. The cascaded form for $Z_\ell(\omega)$ is quite complex. For our calculations we take $\mathrm{Re}[Z_\ell(\omega)] = \sum_i \mathrm{Re}[Z_{RC}^{(i)}]$

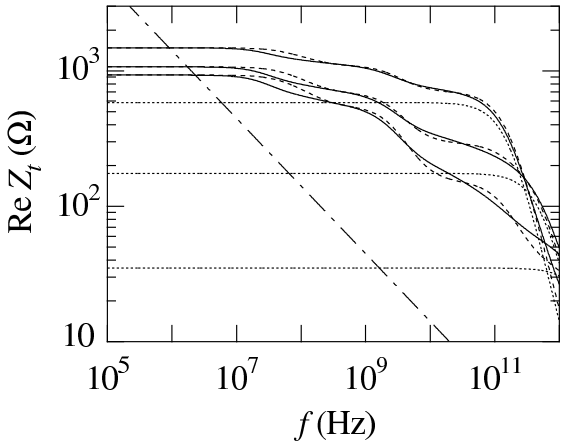

FIG. 3: Calculated $Z_t(\omega)$ for (bottom to top) $Z_{2D} = 258$, 1291 and 4302 Ω for three different models: cascaded RC lines (solid), approximate series combination (dashed) and Z_{2D} only (dotted). The dash-dotted line is the impedance of an infinite line with $r_\ell = 2.9$ MΩ/m and $c_\ell = 23$ nH/m.

where the $Z_{RC}^{(i)}$ are the impedances of the individual sections, a very good approximation to the more exact result, as shown. Note that this model predicts a significant Z_t at 2 GHz dominated by Z_ℓ (Z_{2D}) for small (large) Z_{2D}. For the stripe, Z_{2D} approaches $R_{\rm QPC}/2$ at zero frequency and the much lower stripe resistance $R_{\rm str} \approx 200\ \Omega$ at frequencies above $1/R_{\rm QPC}C_{\rm str}$ where $C_{\rm str} \approx 0.3$ pF is its capacitance to ground. At high frequencies, then, Z_t in the stripe is always dominated by Z_ℓ, even for large negative V_g. We have also shown the impedance for Z_{2D} alone, and for an infinite RC line with $w = 10$ μm and r_ℓ chosen to give the correct $Z_\ell(0)$ if the line were finite. The latter two models give a small Z_t for small Z_{2D} at the relevant frequencies, and cannot explain the linear region in our $V_g = 0$ I-V characteristics.

Using $P_{2D}(E)$ and $P_{RC}(E)$ above, we numerically convolve the $P_i^{(j)}(E)$ for junction j and section i to find $P_\ell^{(j)}(E) = P_1^{(j)}(E) * P_2^{(j)}(E) * P_3^{(j)}(E) * P_4^{(j)}(E)$. We then calculate $P_{\rm tot}^{(j)}(E) = P_\ell^{(j)}(E) * P_{2D}(E)$ for different G_{2D} and set up a master equation using the rates in Eq. 1 to calculate the S-SET current and conductance $G_{\rm SET}^c$. The results for $G_{\rm SET}^c$ in the pool geometry are shown as the solid line in Fig. 2(a); we scale $G_{\rm SET}^c$ to match the maximum measured value $G_{\rm SET}^{\rm max} \approx 0.34G_0$ at $G_{2D}^{\rm max} \approx 6.5G_0$ but use no other variable parameters. $G_{\rm SET}^c$ agrees reasonably well with $G_{\rm SET}$ for $G_{2D} < G_{2D}^{\rm max}$ although it rises less steeply with G_{2D}. In this regime $P_{2D}(E)$ is broad and inelastic transitions suppress the coherent supercurrent. For $G_{2D} > G_{2D}^{\rm max}$, $G_{\rm SET}^c$ gradually saturates at $0.47G_0$. For $G_{2D} \gg G_{2D}^{\rm max}$, $P_{2D}(E) \approx \delta(E)$ (*i. e.*, only elastic transitions are likely) and $P_\ell(E)$ dominates the I-V characteristic. No nonmonotonic behavior occurs in $G_{\rm SET}^c$, in agreement with Wilhelm *et al.* The drop in $G_{\rm SET}$ for $G_{2D} > G_{2D}^{\rm max}$ must arise from other physics.

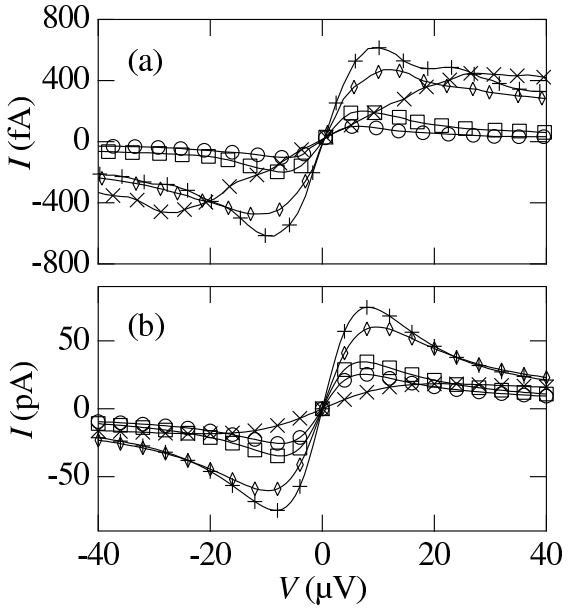

FIG. 4: Measured (a) and calculated (b) I-V characteristics for an unconfined 2DEG (○), $V_g = -0.3$ V (□), and $Z_{2D} = 1613$ (+), 2151 (◇) and 6453 Ω (×). To fit the data at $V_g = 0$ and -0.3 V, we use $\sigma_{ch} = 0.07$ and $0.05e$, respectively. For the remaining curves we take $\sigma_{ch} = 0$.

We can model the drop by assuming that the measured I and $G_{\rm SET}$ are actually averaged over charge states close to n_g, due to charge motion in the substrate [14]. We expect charge averaging to be most pronounced when the 2DEG is unconfined, and least for small G_{2D}. Assuming a Gaussian distribution of charge states with mean n_g and variance σ_{ch}, we calculate the average $\langle G^c_{\rm SET}\rangle$. We do not know the absolute size of σ_{ch}, so we assume for the pool that $\sigma_{ch} = 0$ for $G_{2D} < G^{\rm max}_{2D}$. For $G_{2D} > G^{\rm max}_{2D}$ we find the values of σ_{ch} which give $\langle G^c_{\rm SET}\rangle = G_{\rm SET}$ for the pool and stripe and plot the results in the inset to Fig. 2(a). In both cases σ_{ch} is just below $0.04e$ near $V_g = 0$ V and drops near $V_g = -0.28$ V. For the stripe, σ_{ch} saturates at just above $0.02e$, about half the drop for the pool. The model seems reasonable given the small σ_{ch} required to explain the discrepancies with the environmental theory.

We gain further confidence in the model by comparing measured and calculated I-V characteristics for the pool, as shown in Fig. 4 for S1. For increasing confinement I first rises at all voltages, with little or no broadening of the linear region ($V_g = 0$ and -0.3 V and $Z_{2D} = 1613\,\Omega$). This corresponds to a reduction in σ_{ch} with little change in $P_{\rm tot}(E)$; inelastic transitions in the leads dominate the energy exchange. Eventually, $\sigma_{ch} = 0$ and Z_{2D} is large enough to affect $P_{\rm tot}(E)$, causing I to decrease (especially at low bias) and the linear region to broaden. The level of agreement between the shape and evolution of the measured and calculated curves is surprisingly good, given the uncertainties involved. While the calculated current is much larger than is measured, such discrepancies are common in small tunnel junction systems [14].

In conclusion, we have measured the effects of dissipation on transport in an S-SET for which the environment can be varied locally. We find good agreement with a model in which fluctuations in the leads and low-frequency switching between charge states dominate for low confinement (large G_{2D}), while for strong confinement (small G_{2D}) fluctuations coupled via the capacitance C_{2D} dominate. The model accounts well for the evolution of $G_{\rm SET}$ and the I-V curves as G_{2D} is varied. We believe a convolved $P_{\rm tot} = P_\ell * P_{2D}$ is likely required to interpret the results of the Berkeley group, which may explain the discrepancies between their results and the scaling theory of Wilhelm, *et al.*

This research was supported at Rice by the NSF under Grant No. DMR-9974365 and by the Robert A. Welch foundation, and at UCSB by the QUEST NSF Science and Technology Center. One of us (A. J. R.) acknowledges support from the Alfred P. Sloan Foundation. We thank A. C. Gossard for providing the 2DEG material.

* Current address: Cielo Communications, Inc., 325 Interlocken Parkway, Broomfield, CO 80021.

[1] A. J. Rimberg, T. R. Ho, Ç. Kurdak, J. Clarke, K. L. Campman, and A. C. Gossard, Phys. Rev. Lett. **78**, 2632 (1997).
[2] N. Mason and A. Kapitulnik, Phys. Rev. Lett. **82**, 5341 (1999).
[3] J. S. Penttilä, Ü. Parts, P. J. Hakonen, M. A. Paalanen, and E. B. Sonin, Phys. Rev. Lett. **82**, 1004 (1999).
[4] Y. Nakamura, Yu. A. Pashkin, and J. S. Tsai, Nature **398**, 786 (1999).
[5] V. Bouchiat, D. Vion, P. Joyez, D. Esteve, and M. H. Devoret, Phys. Scripta **T76**, 165 (1998).
[6] Yu. Makhlin, G. Schön, and A. Shnirman, Nature **398**, 305 (1999).
[7] J. B. Kycia, J. Chen, R. Therrien, Ç. Kurdak, K. L. Campman, A. C. Gossard, and J. Clarke, Phys. Rev. Lett. **87**, 017002 (2001).
[8] M. H. Devoret, D. Esteve, H. Grabert, G.-L. Ingold, H. Pothier, and C. Urbina, Phys. Rev. Lett. **64**, 1824 (1990).
[9] G.-L. Ingold and Yu. V. Nazarov, in *Single Charge Tunneling*, edited by H. Grabert and M. H. Devoret (Plenum, New York, 1992), pp. 21–107.
[10] H. Grabert, G.-L. Ingold, and B. Paul, Europhys. Lett. **44**, 360 (1998).
[11] T. Dittrich, P. Hänggi, G.-L. Ingold, B. Kramer, G. Schön, and W. Zwerger, *Quantum Transport and Dissipation* (Wiley-VCH, Weinheim, Germany, 1998).
[12] G.-L. Ingold and H. Grabert, Phys. Rev. Lett. **83**, 3721 (1999).
[13] F. K. Wilhelm, G. Schön, and G. T. Zimányi, Phys. Rev. Lett. **87**, 136802 (2001).
[14] T. M. Eiles and J. M. Martinis, Phys. Rev. B **50**, 627 (1994).
[15] W. Lu, A. J. Rimberg, K. D. Maranowski, and A. C.

Gossard, Appl. Phys. Lett. **77**, 2746 (2000).
[16] A. A. Odintsov, G. Falci, and G. Schön, Phys. Rev. B **44**, 13 089 (1991).
[17] G.-L. Ingold, P. Wyrowski, and H. Grabert, Z. Phys. B **85**, 443 (1991).
[18] W. Lu, K. D. Maranowski, and A. J. Rimberg, Phys. Rev. B **65**, 060501 (2002).
[19] D. V. Averin, Yu. V. Nazarov, and A. A. Odintsov, Physica B **165&166**, 945 (1990).